3-22-1999

Spatio-Temporal Growth of Nematic Domains in Liquid Crystal Polymer Mixtures

Hao-Wen Chiu
University of Akron Main Campus

Thein Kyu
University of Akron Main Campus, tkyu@uakron.edu

Spatio–temporal growth of nematic domains in liquid crystal polymer mixtures

Hao-Wen Chiu and Thein Kyu[a)]
Institute of Polymer Engineering, University of Akron, Akron, Ohio 44325-0301

(Received 20 October 1998; accepted 28 December 1998)

Dynamics of phase separation and morphology development in mixtures of a low molar mass liquid crystal (LC) and a polymer have been investigated theoretically in comparison with experimental results. In the theoretical model, the combined free-energy densities of Flory–Huggins theory for isotropic mixing and Maier–Saupe theory for nematic ordering have been incorporated into the time-dependent Ginzburg–Landau equation (type C). The temporal evolution of the structure factor and the emergence of phase-separated liquid crystal domains have been simulated on the basis of an explicit central difference method based on a square lattice (128×128) with a periodic boundary condition. Of particular interest is the observed plateau (or inflection) region in the growth dynamic curve, which may be attributed to the breakdown of the interconnected domains caused by the nematic ordering. This unique behavior has been verified experimentally in terms of the growth of structure factor following several temperature quenches into a nematic+liquid region of the experimental phase diagram of an *E*7/poly(methyl methacrylate) mixture. Further, the emergence of LC domains in the metastable and unstable nematic–liquid spinodal regions has been investigated theoretically and compared with the reported experimental results. © *1999 American Institute of Physics.* [S0021-9606(99)52012-6]

I. INTRODUCTION

The morphology of liquid crystal (LC) dispersions in liquid crystal/polymer composite films such as polymer-dispersed liquid crystal (PDLC) and polymer-stabilized liquid crystal (PSLC) is of crucial importance for successful applications in electro-optical devices.[1,2] These composite films are generally produced either through thermal quenching or photopolymerization of the reactive matrix binder. In the former case of thermally induced phase separation (TIPS), the instability of the PDLC system is driven by the competition between phase separation and nematic ordering. As for the latter case, the instability is caused by an increase in molecular weight of the starting reactive monomers that eventually induces phase separation. This process is often referred to as polymerization-induced phase separation (PIPS).[3]

In previous papers,[4–8] we have established theoretical phase diagrams of various LC/polymer mixtures by solving self-consistently the combined Flory–Huggins (FH) equation for isotropic mixing, Maier–Saupe (MS) theory for nematic ordering, or Maier–Saupe–McMillan (MSM) theory for smectic ordering. These binary systems include nematic/polymer,[4] two nematics,[5] smectic/polymer,[6] two smectics[7] and nematic/smectic mixtures.[8] The phase diagram of nematic/nematic mixtures exhibits various coexistence regions such as liquid+liquid, nematic+liquid, nematic +nematic in the middle compositions, and the pure nematics at the high compositions of either component. In the binary smectics,[7] the phase diagram consists of liquid+liquid, nematic+smectic, and smectic+smectic at the intermediate compositions, and the pure smectic regions at the extremely high composition of either component. These predicted coexistence regions have been confirmed experimentally. It has been recognized that the final LC domain morphology depends not only on thermodynamic phase equilibria of the LC/polymer mixtures, but also depends strongly on dynamics of phase decomposition and nematic ordering, as most polymer systems hardly reach an equilibrium state.[9,10]

As a continuing effort, we turn our attention to elucidate the morphology development and determine the dynamics of phase transitions in nematic/polymer mixtures. To mimic the emergence of nematic domain morphology, the time-dependent Ginzburg–Landau (TDGL) equations,[9–14] ''Model C,'' have been adopted by incorporating the spatio–temporal evolution of the conserved density (or concentration) order parameter of the LC and that of the nonconserved orientational order parameter of the LC directors.[13] The two-coupled TDGL equations have been solved numerically by incorporating the combined Flory–Huggins theory for isotropic mixing[15,16] and Maier–Saupe theory for nematic ordering.[17,18] Of particular interest is the observed plateau region in the coarsening dynamic curves caused by the nematic ordering. This unusual plateau region is consistent with our experimental results of blends of nematic LC/poly(methyl methacrylate) obtained previously by light scattering.[19,20] The emergence of the domain morphology in nematic/polymer composite films has been investigated by means of optical microscopy, following several thermal quenches from a single phase to various coexistence regions. The calculated domain morphologies have been compared with the observed LC domain textures.

[a)]Author to whom correspondence should be addressed.

II. MODEL DESCRIPTION

The emergence of liquid crystal (LC) domains in a polymer dispersed liquid crystal system is generally controlled by a competition between liquid–liquid phase separation and nematic ordering. The dynamics of such a dissipative system may be described in terms of the coupled time-dependent Ginzburg–Landau (TDGL) equations,[9–14] i.e., ''Model C'' in which a conserved order parameter, i.e., the volume fraction of the liquid crystals (LC), is coupled with a nonconserved orientational order parameter. These two-coupled equations have been expressed customarily as

$$\frac{\partial \phi(r,t)}{\partial t} = \nabla \cdot \left[\Lambda \nabla \left(\frac{\delta G}{\delta \phi} \right) \right] + \eta_\phi(r,t), \tag{1}$$

$$\frac{\partial s(r,t)}{\partial t} = -R \left(\frac{\delta G}{\delta s} \right) + \eta_s(r,t), \tag{2}$$

where $\phi(r,t)$ and $s(r,t)$ represent the volume fraction and the orientation order parameter of the LC component at position r and time t, respectively. Λ is defined as the mutual diffusion coefficient having the property of the Onsager reciprocity.[21] R is the rotational mobility of the LC molecules.[13] The concentration and orientation fluctuations, η_ϕ and η_s are customarily expressed according to the fluctuation-dissipation theorem as

$$\langle \eta_\phi(r,t)\, \eta_\phi(r',t') \rangle = -2k_B T \Lambda \nabla^2 \delta(r-r')\, \delta(t-t'), \tag{3}$$

$$\langle \eta_s(r,t)\, \eta_s(r',t') \rangle = 2k_B T R\, \delta(r-r')\, \delta(t-t'), \tag{4}$$

in which k_B is the Boltzmann constant and T is temperature.

The mutual diffusion coefficient Λ, for a binary system, is generally given by

$$\Lambda = \frac{\Lambda_1 \Lambda_2}{\Lambda_1 + \Lambda_2}, \tag{5}$$

where $\Lambda_1 = \phi N_1 D_1$ and $\Lambda_2 = (1-\phi) N_2 D_2$ in which N_1 represents the degree of polymerization of the dispersing liquid crystals and N_2 is that of the matrix polymer. D_1 and D_2 are the self-diffusion coefficients of the LC molecules and the polymer chains, respectively. In the framework of reptation theory,[22] it may be expressed as

$$D_j = \frac{k_B T}{\zeta_j} \frac{N_{e,j}}{N_j^2}, \tag{6}$$

where $j = 1$ or 2. Here, ζ_j and $N_{e,j}$ are the frictional coefficient per monomer unit and the distance between the entanglements of component j, respectively.

The total free-energy of the system, G, is given by the integration of the local free-energy density over all volume, viz.,

$$\frac{G}{k_B T} = \int_V (g^i + g^n + \kappa_\phi |\nabla \phi|^2 + \kappa_s |\nabla s|^2) dV, \tag{7}$$

where g^i is the free-energy density of isotropic mixing and g^n is the free-energy density due to the anisotropic ordering of the LC molecules. $\kappa_\phi |\nabla \phi|^2$ is the free-energy contribution of the concentration gradient in which κ_ϕ is a coefficient relating to the segmental correlation length and the local concentration. For an asymmetric polymer–polymer mixture[23]

$$\kappa_\phi = \tfrac{1}{36} \left[\frac{a_1^2}{\phi_1} + \frac{a_2^2}{\phi_2} \right], \tag{8}$$

where a_1 and a_2 are the correlation lengths of polymer segments of the component 1 and 2, respectively. The $\kappa_s |\nabla s|^2$ term in Eq. (7) represents the gradient of the free-energy of the orientation order parameter. For simplicity, κ_s may be taken as constant.

The isotropic part of the free-energy is generally described in term of the Flory–Huggins (FH) theory,[15,16] i.e.,

$$g^i = \frac{\phi}{N_1} \ln \phi + \frac{(1-\phi)}{N_2} \ln(1-\phi) + \chi \phi (1-\phi), \tag{9}$$

where χ is the Flory–Huggins interaction parameter defined as $\chi = A + B/T$ with A and B being constants.[16]

The anisotropic part of the free energy may be given according to the Maier–Saupe (MS) theory[17,18]

$$g^n = \tfrac{1}{2} \nu s^2 \phi^2 - \phi \ln Z, \tag{10}$$

where ν is the nematic interaction parameter defined as $\nu = 4.541 (T_{NI}/T)$[4,5] in which T_{NI} is the nematic–isotropic (NI) transition temperature of the LC component. Z is the partition function given as

$$Z = \int_0^1 e^{\nu s \phi (\frac{3}{2} \cos^2 \theta - \frac{1}{2})} d \cos \theta, \tag{11}$$

and s is the nematic order parameter defined as

$$s = \tfrac{1}{2} \langle 3 \cos^2 \theta - 1 \rangle = \frac{\int_0^1 (\frac{3}{2} \cos \theta - \frac{1}{2}) e^{\nu s \phi (\frac{3}{2} \cos \theta - \frac{1}{2})} d \cos \theta}{Z}. \tag{12}$$

Based on the combined FH/MS free energy expression, Eqs. (1) and (2) becomes

$$\frac{\partial \phi}{\partial t} = \nabla \cdot \left[\Lambda \nabla \left(\frac{\partial g^i}{\partial \phi} + \frac{\partial g^n}{\partial \phi} - \kappa_\phi \nabla^2 \phi \right) \right] + \eta_\phi, \tag{13}$$

$$\frac{\partial s}{\partial t} = -R \left(\frac{\partial g^n}{\partial s} - \kappa_s \nabla^2 s \right) + \eta_s, \tag{14}$$

where

$$\frac{\partial g^i}{\partial \phi} = \frac{\ln \phi + 1}{N_1} - \frac{\ln(1-\phi) + 1}{N_2} + \chi (1 - 2\phi), \tag{15}$$

$$\frac{\partial g^n}{\partial \phi} = \nu s^2 \phi - \ln Z - \phi \frac{\partial \ln Z}{\partial \phi}, \tag{16}$$

$$\frac{\partial g^n}{\partial s} = \nu s \phi^2 - \phi \frac{\partial \ln Z}{\partial s}. \tag{17}$$

The pattern-forming aspects of phase separation within a PDLC system may be investigated by numerically solving Eqs. (13) and (14). The calculation was performed on a two-dimensional square lattice (128×128) using an explicit method for temporal steps and a central difference scheme for spatial steps with a periodic boundary condition. The

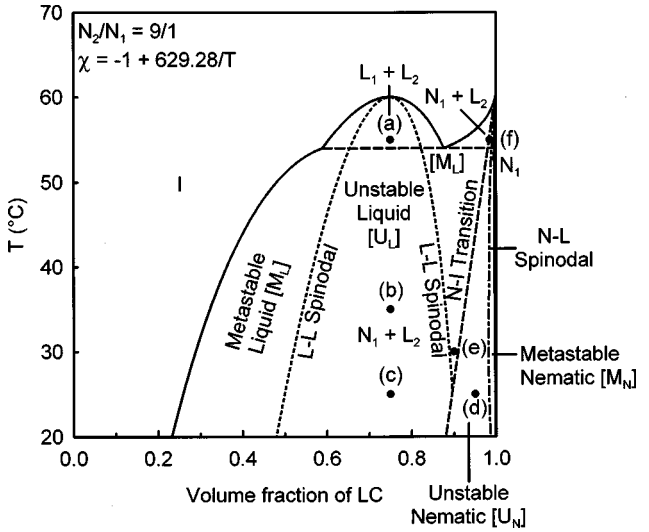

FIG. 1. A hypothetical phase diagram of a polymer/nematic liquid crystal mixture, calculated on the basis of the combined FH/MS theory, displaying various coexistence regions. Regions (a)–(f) indicate various temperature quenches performed at different compositions.

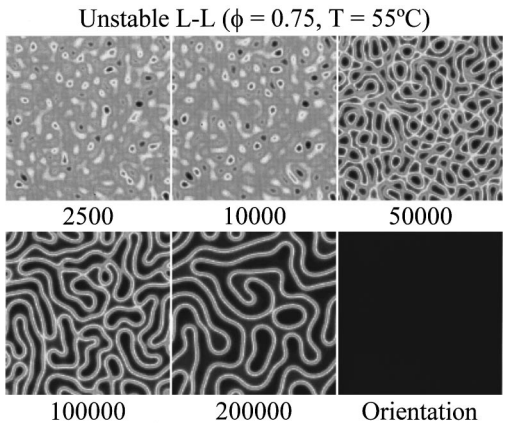

FIG. 2. Temporal evolution of the compositional order parameter for a T quench into the liquid–liquid coexistence region (a) in Fig. 1, where $T=55\,^{\circ}\mathrm{C}$ and $\phi=0.75$. The calculation was performed using the following parameters: $D_1=9$, $D_2=1$, $a_1=0.6$, $a_2=0.6$, $R=1$, and $\kappa_s=0.001$.

temporal evolution of structure factors, $S_\phi(q,t)$ and $S_s(q,t)$, may be determined by rewriting Eqs. (13) and (14) in a Fourier space, i.e.,

$$S_\phi(q,t)=F[\phi(r_1,t)\phi(r_2,t)], \tag{18}$$

$$S_s(q,t)=F[s(r_1,t)s(r_2,t)], \tag{19}$$

where F represents the Fourier transformation and q is the scattering wave number defined as $q=[4\pi/\lambda]\sin(\theta/2)$ where λ and θ are the wavelength of incident light and scattering angle in the medium, respectively. Comparing the temporal change of the calculated structure factors with the experimental results of the time-resolved scattering studies, the validity of Eqs. (18) and (19) may be tested.

III. RESULTS AND DISCUSSION

A. Phase diagram and coexistence regions

Figure 1 illustrates a typical phase diagram of a polymer/nematic liquid crystal mixture calculated on the basis of the combined FH/MS theory[4,5] using the following conditions: $T_{\mathrm{NI}}=60\,^{\circ}\mathrm{C}$, the critical composition of liquid–liquid phase separation $\phi_c=0.75$ corresponding to $N_2/N_1=9/1$, and the critical temperature $T_c=60\,^{\circ}\mathrm{C}$. The constant A of χ parameter is set as $A=-1$, which in turn gives $B=629.28$ from the criticality condition, i.e., $\chi=A+\{(\chi_c-A)/T_c\}/T$. The calculated phase diagram is basically an overlap of an upper critical solution temperature (UCST) and a nematic–isotropic transition, exhibiting a variety of coexistence regions such as liquid+liquid and nematic (N)+liquid (L) in the intermediate compositions. In the very high LC-rich compositions, the pure nematic and a narrow $N+L$ region exists at high temperatures in the high-LC composition. Following the method of Shen and Kyu,[4] the nematic spinodal line has been calculated self-consistently as depicted in Fig. 1. The nematic spinodal line further divides the narrow $N+L$ region into the metastable nematic and the unstable nematic regions. As labeled in the phase diagram, the metastable nematic region is bound by the pure nematic and the nematic spinodal lines, whereas the unstable nematic region is bound by the nematic spinodal and the nematic–isotropic transition lines. Regarding the detailed calculations of the phase diagram, interested readers are referred to our previous papers.[4,5] More importantly, a similar polymer/nematic phase diagram has been observed experimentally for the PMMA/$E7$ and PMMA–OH/$E7$ systems.[19,20]

B. Temperature quench into liquid+liquid coexistence region

Having established the thermodynamic phase diagram of the polymer/nematic liquid crystals, it is of natural interest to explore the dynamic aspects of phase separation and nematic ordering within these regions. The emergence of domain morphologies has been first calculated for the critical composition in order to simulate a temperature (T) quench experiment into the $L+L$ coexistence region, e.g., 55 °C [i.e., at region (a)]. Figure 2 shows the temporal evolution of the compositional order parameter (or volume fraction), depicting the emergence of the bicontinuous domain morphology reminiscent of spinodal decomposition (SD). As expected, the analogous orientational order parameter shows no texture, as the liquid crystals are practically in the isotropic state (see the picture at 200 000 steps in Fig. 2). With elapsed time, the SD domains grow via coalescence. The interface boundaries are not clearly discernible in the early period of phase separation (10 000 steps), but become distinct in the later times, exhibiting the distinct concentration gradient (e.g., see 50 000 to 200 000 steps). This observation is consistent with the conventional liquid–liquid phase separation in binary polymer blends.

Fourier transformation was carried out to obtain the structure factor analogous to the scattering wave number maximum. The temporal evolution of the scattering patterns, as obtained by Fourier transforming the domain structure of Fig. 2, is depicted in Fig. 3. Initially, the scattering is seemingly dominated by the thermal fluctuations, followed by the development of a broad and weak scattering halo. The ap-

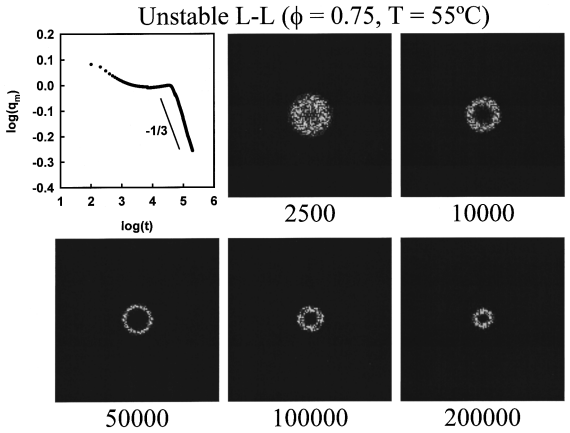

FIG. 3. Temporal evolution of the compositional structure factor as obtained by Fourier transforming the domain structure of Fig. 2.

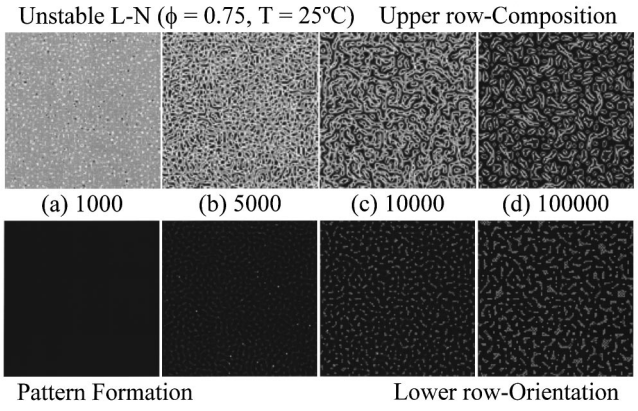

FIG. 4. Temporal evolutions of compositional order parameter (upper row) and orientational order parameter (lower row) at a critical quench of 25 °C into the nematic–liquid coexistence region (c) in Fig. 1. The calculation was performed using the following parameters: $D_1=1.8$ and $D_2=0.2$. Other parameters are kept the same as those in Fig. 2.

pearance of the scattering halo suggests the development of domain periodicity. This diffused scattering halo collapses into a smaller diameter while becoming sharper. Concurrently, the intensity increases immensely, which may be attributed to the coalescence of the domains.

The growth dynamics of the phase-separated domains is analyzed customarily in terms of a power law, i.e.,

$$q_m(t)=\xi(t)^{-1}\propto t^{-\alpha}, \tag{20}$$

where the scattering wave number maximum, q_m, is defined as $q_m=(4\pi/\lambda)\sin\theta_m/2$, ξ represents the length scale or domain size, and α is the growth exponent. To quantify the change in length scale (or domain size), the scattering maxima were plotted against elapsed time in a double logarithmic form in Fig. 3. In the early period, the structure factor is virtually invariant, suggestive of spinodal decomposition (SD). In the intermediate stage, the structure factor decreases rapidly with a slope of $-1/3$ due to the coalescence of the SD domains. These features are familiar characteristics of the liquid–liquid phase separation via spinodal decomposition at a critical quench. As will be discussed later, the crossover of the growth exponent from $-1/3$ to -1 is discernible only when the T quench is sufficiently deep into the unstable liquid+liquid coexistence region. In the present case, the deep T quench experiments will lead to the nematic–liquid phase separation; thus, the growth behavior is expected to be different from the conventional isotropic liquid–isotropic liquid phase separation.

C. Temperature quench into a nematic–liquid coexistence region

The T-quenches into the $N+L$ region show several noteworthy features. Figure 4 shows the temporal evolution of the compositional order parameter (upper row) and of the orientational order parameter (lower row) at a critical quench to 25 °C [region (c) in the phase diagram of Fig. 1]. Tiny multiple domains emerge instantaneously from the concentration fluctuation. However, the orientational order parameter shows no texture in the corresponding initial period of 1000 steps. With elapsed time, the structures in the concentration field (i.e., the compositional order parameter) evolve into the interconnected texture suggestive of phase separation via spinodal decomposition. Concurrently, the nematic ordering takes place within the interconnected domains as shown in the orientational order parameter field at 5000 steps. The interconnected domains further grow in size via coalescence, and the orientational ordering increases subsequently within these growing domains ($t=5000$). With elapsed time, these interconnected structures eventually break down into smaller domains while transforming gradually into a droplet shape (see the upper row at $t=100\,000$). It should be emphasized that such a pattern-forming process has been observed experimentally in a PMMA–OH/$E7$ mixture reported earlier (see Fig. 5 of Ref. 20).

As mentioned before, the morphology emerging process in a polymer dispersed liquid crystal system involves a competition between the liquid–liquid phase separation and the nematic ordering. According to the combined FH/MS theory,[4,5] nematic ordering will occur only when the concentration of the liquid crystals exceeds the critical concentration $\phi_{\mathrm{NI}}=T/T_{\mathrm{NI}}$. During the initial stage, the phase separation process is mainly driven by liquid–liquid SD due to the fact that the LC concentration in the phase-separated do-

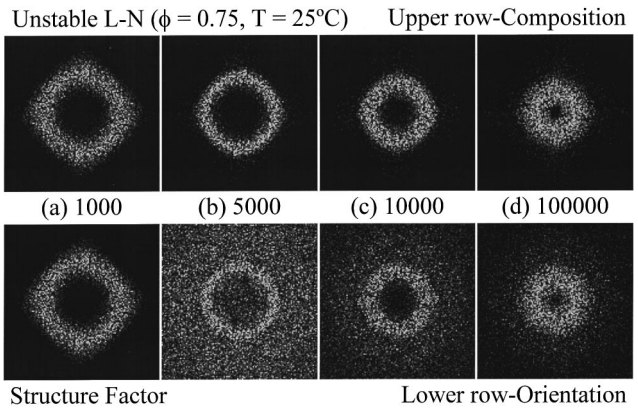

FIG. 5. Temporal evolutions of the compositional structure factor (upper row) and orientational structure factor (lower row) as obtained by Fourier transforming the domain structure of Fig. 4.

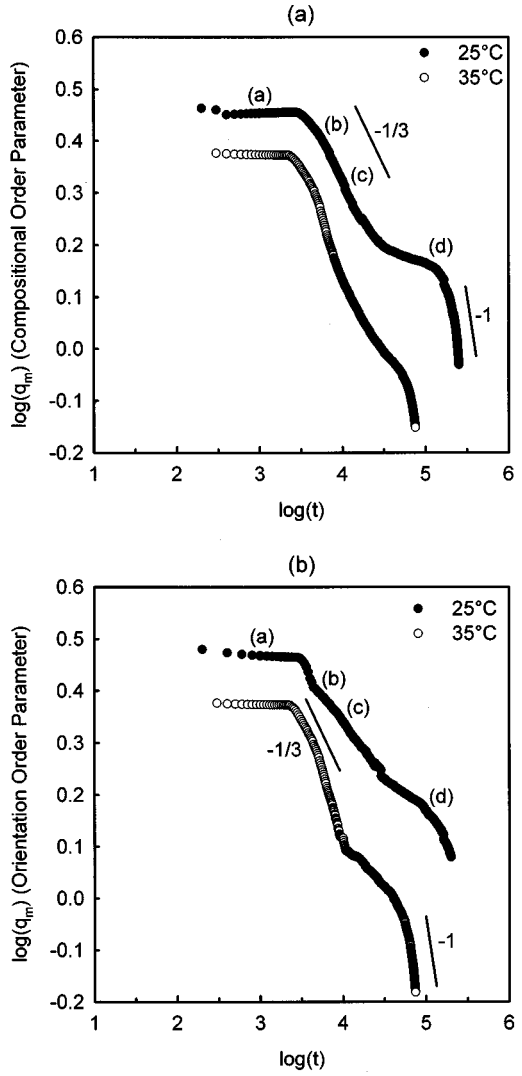

FIG. 6. Temporal evolution of the scattering wave number maximum corresponding to the growth of length scale for (a) the compositional order parameter from Fig. 4 (upper row), and (b) the orientational order parameter from Fig. 4 (lower row).

mains has yet to reach the critical concentration, ϕ_{NI}. In the intermediate stage, nematic ordering occurs within the interconnected domains as the LC concentration reaches ϕ_{NI}. The liquid–liquid phase separation is probably still dominant over the nematic ordering in the early and intermediate periods. For the late stage of phase separation, the spinodal structures break down and transform into the droplet-like domains that may be attributed to the instability driven by the dominant nematic ordering. Although the gradient of the interface boundary is clearly discernible in the compositional order parameter (hereafter called the concentration field), there is virtually no gradient in the interface boundary in the orientational order parameter (abbreviated as the orientation field). Recall that in the Maier–Saupe theory,[17,18] the nematic structure can form only when the orientational order parameter (s) exceeds a critical value of $s_c = 0.429$. It appears that LC and polymer chains are presumably mixed at various extents such that a concentration gradient may develop at the interface. Due to this mixing, there will be no nematic ordering for any s value less than 0.429; hence, the orientational order parameter will undergo abrupt change at the interface. Consequently, the boundary appears sharp in the orientation field.

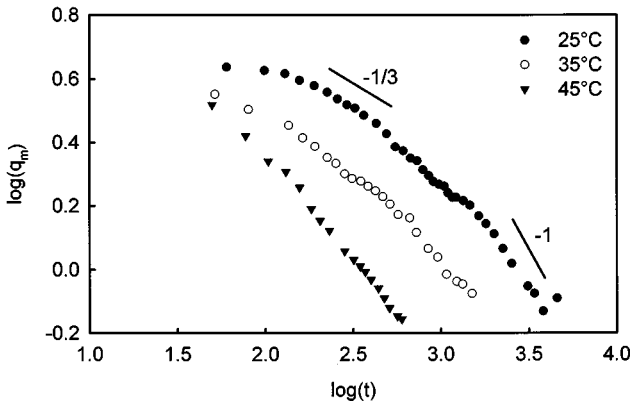

FIG. 7. Temporal evolution of scattering wave number maximum for the 60/40 *E*7/PMMA mixture obtained by time-resolved light scattering.

To mimic the growth of the structure factors, Fourier transformation was undertaken on the emerging domain structures resulting in the scattering patterns. As shown in Fig. 5, the scattering halo is a typical signature of phase separation via spinodal decomposition. Of particular interest is the revelation of diffused scattering overlapping with the existing scattering halo (see $t = 5000$ in the orientational field). This diffused scattering is believed to arise from the interference among the nematic structures that are emerging within the preformed interconnected SD domains (see Fig. 4). As the nematic structure begins to volume-fill in the preformed SD domains, the diffused scattering diminishes gradually and eventually emerges with the scattering halo arising from the concentration fluctuations.

The scaling behavior of the growth dynamics has been analyzed in terms of the temporal evolution of the scattering maxima in both concentration and orientation fields. Figures 6(a) and (b) show the growth curves for temperature quenches to 25 and 35 °C along with the labeled regions (a–d) corresponding to the emerging structures and scattering patterns of Figs. 4 and 5. As can be seen in Fig. 6(a), the temporal evolution of the scattering maximum for the concentration field initially follows a power law of $-1/3$, then crosses over to the -1 regime, where the hydrodynamic effect becomes dominant. In the crossover regime, it is striking to discern a plateau (or inflection) region corresponding to the onset of the breakdown of the interconnected structure [in Fig. 4, region (d)]. The plateau is more pronounced for the deeper T quench (25 °C) relative to the shallow case (35 °C) [Figure 6(b)]. It appears that liquid–liquid phase separation initially predominates over the nematic ordering in the deeper quench. Subsequently, the nematic ordering probably drives the system to be unstable, leading to the breakdown of the interconnected domains. This crossover region is identifiable in the temporal evolution of the scattering maximum for the orientation field shown in Fig. 6(b).

The existence of a plateau in the growth dynamic plot can be verified experimentally.[19,20] Figure 7 shows the temporal evolution of scattering wave number maximum for the

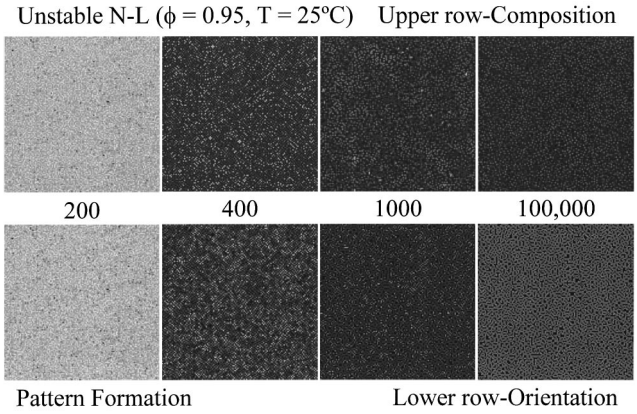

FIG. 8. Temporal evolutions of compositional order parameter (upper row) and orientational order parameter (lower row) for a T quench into the unstable nematic region (d) in Fig. 1, where $T=25\,^{\circ}\mathrm{C}$ and $\phi=0.95$. The calculation was performed with the following parameters: $D_1=1.8$ and $D_2=0.2$. Other parameters are kept the same as those in Fig. 2.

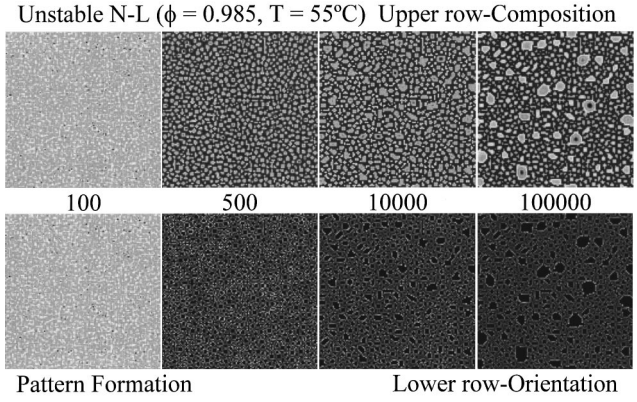

FIG. 9. Temporal evolutions of compositional order parameter (upper row) and orientational order parameter (lower row) for a T quench into the unstable nematic region (f) in Fig. 1, where $T=55\,^{\circ}\mathrm{C}$ and $\phi=0.985$. The calculation was performed using the following parameters: $D_1=9$ and $D_2=1$. Other parameters are kept the same as those in Fig. 2.

60/40 $E7$/PMMA obtained by time-resolved light scattering.[19] The T quench experiment was undertaken from a single-phase temperature of 93 °C to various temperatures within the $N+L$ coexistence region. The inflection can be discerned at deep quenches to 25 and 35 °C. However, it is no longer discernible at 45 °C. In the original paper, the significance of the inflection was not realized, and therefore the lines were drawn through these inflection regions. In another dynamic study on the $E7$/PMMA–OH system,[20] a similar inflection was observed in the growth curve. It is reasonable to infer that the present calculation, based on the coupled TDGL equations (type C) in conjunction with the combined FH/MS theory, truly captures the experimental trend of the growth dynamics of liquid crystal domains.

D. Temperature quench into an unstable nematic–liquid region

The prediction of the nematic–liquid ($N-L$) spinodal[4] line is not only important in the establishment of phase diagram of polymer/liquid crystal mixtures, but also opens up a new avenue pertaining to development of a nematic spinodal structure. To the best of our knowledge, the experimental verification of such an $N-L$ spinodal region in thermodynamic phase diagrams and the dynamic aspect of phase separation via the $N-L$ spinodal decomposition remain unexplored; therefore, a challenging problem. In order to demonstrate the existence of such an $N-L$ spinodal line and to characterize the structure growth driven by the nematic spinodal mechanism, the emergence of the LC domain structures following several T quenches into the unstable nematic–liquid coexistence regions has been calculated based on the aforementioned TDGL equations, along with the combined FH/MS theory.

Figure 8 shows the temporal evolutions of compositional (upper row) and orientational (lower row) order parameters for a T quench into the unstable nematic region (d) in Fig. 1 where $T=25\,^{\circ}\mathrm{C}$ and $\phi=0.95$. Tiny multiple domains form instantaneously and subsequently evolve into the interconnected texture with elapsed time, suggestive of phase separation via spinodal decomposition. Since the T quench performed is outside the envelope of the liquid–liquid spinodal, phase separation must be induced by the nematic ordering of the LC molecules. There is little or no difference in the textures between the concentration and orientation fields. The length scale (or the SD domain size) in the present off-critical quench into the unstable nematic region is small as compared to those of the critical quench to the region (c). This difference may be attributed to the domination of the nematic ordering over the phase separation in the unstable nematic region. Hence, it is reasonable to conclude that the bicontinuous structures thus formed in the unstable nematic region (d) are due to the nematic–liquid spinodal decomposition.

To further confirm the existence of the $N-L$ spinodal, another T quench has been undertaken into the unstable nematic region at $T=55\,^{\circ}\mathrm{C}$ and $\phi=0.985$, i.e., region (f) in Fig. 1. This region corresponds to the border of the metastable liquid and unstable nematics. Figure 9 shows the calculated temporal evolutions of compositional (upper row) and orientational (lower row) order parameters. The interconnected texture formed initially ($t=100$) is reminiscent of a spinodal structure. The length scale of percolated structure increases with elapsed time, and eventually transforms into droplet morphology ($t=500$), suggesting a transition from a nematic–liquid spinodal to a cluster regime. The LC droplet structure grows in size with elapsed time, while the background matrix retains the bicontinuous structure ($t=10\,000$). Later, the interconnected structure is totally masked under the LC droplet textures due to the dominant appearance of the droplet structure ($t=100\,000$).

To verify the coexistence of the droplet morphology and the spinodal texture, Fourier transformation of the domain structures was performed to discern the difference in the length scales of the two structures. Figure 10 shows the temporal evolution of the corresponding scattering patterns obtained by Fourier transforming the domain structures of Fig. 9. The structure factors of the concentration (upper row) and orientation (lower row) order parameters both initially show a scattering ring, suggestive of a spinodal decomposition

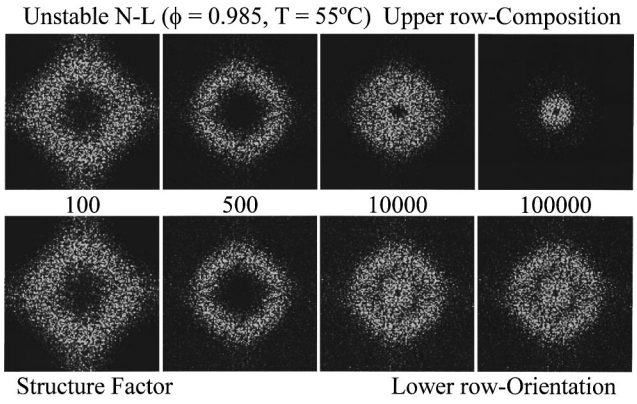

FIG. 10. Temporal evolutions of the compositional structure factor (upper row) and orientational structure factor (lower row) as obtained by Fourier transforming the domain structure of Fig. 9.

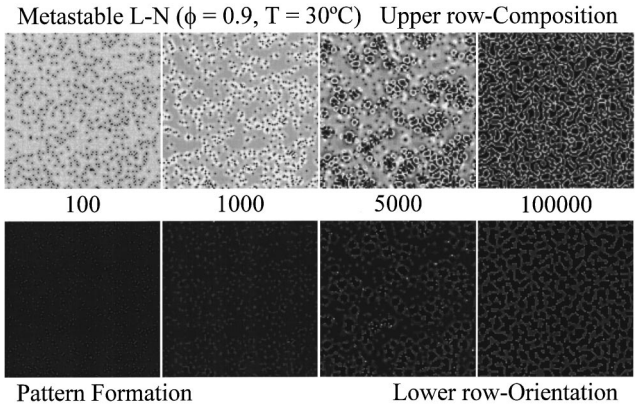

FIG. 12. Temporal evolutions of compositional order parameter (upper row) and orientational order parameter (lower row) for a T quench into the metastable liquid–nematic region (e) in Fig. 1, where $T=30\,^{\circ}\mathrm{C}$ and $\phi=0.9$. The calculation was performed using the following parameters: $D_1=3.6$ and $D_2=0.4$. Other parameters are kept the same as those in Fig. 2.

(e.g., see $t=100$). Later, a second scattering halo appears at the center ($t=10\,000$) corresponding to the dispersion of tiny LC droplets within the interconnected domains. Subsequently, these LC droplets grow in size and eventually fill the entire interconnected domains, resulting in the fading of the outer scattering ring ($t=100\,000$). Nevertheless, the coexistence of the two scattering rings for the orientation field permits the investigation of the growth of both structures separately. The temporal evolution of average length scales for the two structures in the concentration and orientation fields may be characterized by the evolution of the corresponding scattering maxima. As illustrated in Fig. 11, the progression of the scattering maximum for the interconnected texture, i.e., the outer ring of the scattering pattern, initially follows a power law of $-1/3$, then levels off. The temporal evolution of the length scale for the LC droplets, i.e., the second peak in the scattering pattern, also follows the $-1/3$ law. The coexistence of the dual scattering maximums suggests the existence of droplet dispersions within the interconnected spinodal texture.

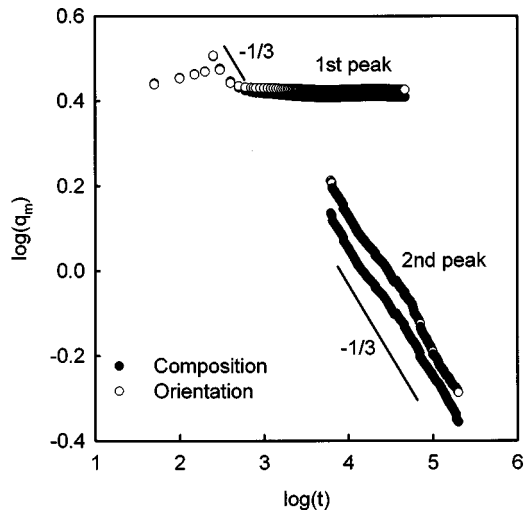

FIG. 11. Temporal evolution of the scattering wave number maximum corresponding to the growth of the domain structures shown in Fig. 9.

E. Temperature quench into a metastable liquid–nematic region

One important characteristic of a metastable region is that it is unstable against large fluctuations. In order for the phase separation to occur in the metastable region (bound by the $L-L$ spinodal and the $N-I$ transition lines), it is necessary to introduce a sufficiently large thermal noise into the system. To simulate the domain-forming process within such a metastable region, a temperature quench was performed into the metastable liquid–nematic region at $T=30\,^{\circ}\mathrm{C}$ and $\phi=0.90$, i.e., region (e) in Fig. 1. Figure 12 shows the corresponding temporal evolutions of the compositional order parameter (upper row) and orientational order parameter (lower row). Tiny droplets form instantaneously within a bicontinuous matrix ($t=100$) and subsequently coarsen ($t=1000-5000$), which is a typical characteristic of nucleation and growth (NG). Concurrently, the bicontinuous structure, reminiscent of a spinodal texture, appears in the background matrix and evolves via coalescence ($t=1000-5000$). Eventually, the domain structure transforms into interconnected domain structure everywhere, suggestive of spinodal decomposition ($t=100\,000$). Hence, the growth of the domain structure is characterized seemingly by a crossover from the NG to SD through the coexistence of NG and SD. It should be pointed out that the overlapped NG/SD structure is nonequilibrium in character; that is to say, it is observable only in the nonequilibrium and nonlinear dynamical process. This crossover behavior can be further verified from the temporal evolution of structure factors.

Figure 13 depicts the scattering patterns corresponding to the domain structures in Fig. 12. The concentration structure factor (upper row) initially shows a spinodal ring overlapping with a diffused scattering pattern at the center ($t=100$), which suggests the coexistence of SD and NG. The outer scattering ring collapses into a smaller diameter while the intensity increases ($t=1000-5000$), which may be attributed to the growth of the interconnected SD structure. Concurrently, the size of the inner scattering pattern reduces due to the growth of the droplet domain. Ultimately, the

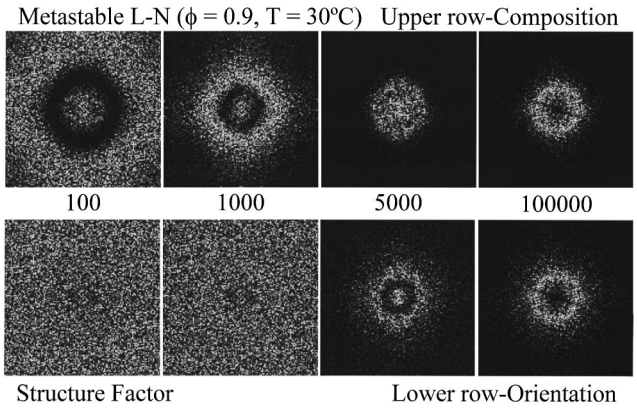

FIG. 13. Temporal evolutions of the compositional structure factor (upper row) and orientational structure factor (lower row) as obtained by Fourier transforming the domain structures of Fig. 12.

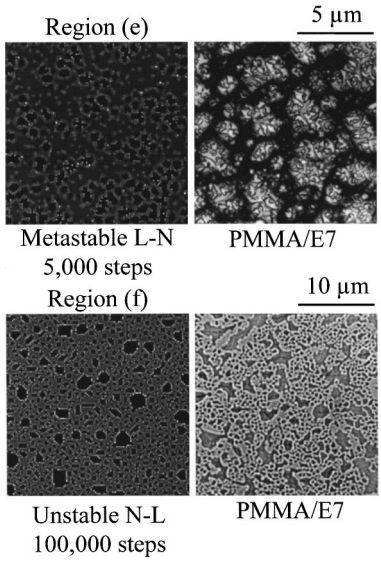

FIG. 14. Comparison between the calculated patterns and experimental observation, showing remarkable similarity.

inner scattering pattern disappears, leaving only the spinodal ring, which in turn suggests the crossover process from NG and SD to SD through the coexistence of NG and SD ($t = 100\,000$). On the other hand, the structure factor due to orientation of the LC directors initially shows only a very diffused pattern without any clear maximum, suggestive of a nucleation and growth process ($t = 100-1000$). The absence of a scattering ring implies the lack of periodicity in the domain structure. At $t = 5000$, the coexistence of a spinodal ring corresponding to SD and a diffused scattering pattern at the center corresponding to NG can be discerned clearly. Later, only the spinodal ring exists in the scattering pattern since the domain structure has transformed completely into the interconnected domains, indicating the crossover from NG to SD via the coexistence of NG and SD. Such a crossover behavior probably depends on the competition between the NG and SD as the system was thrust into the unstable state through a metastable state.

F. Comparison with experiments

To evaluate the predictive capability of the present theory, it is imperative to test with the experimentally observed structures. Figure 14 depicts a comparison between the calculated patterns and experimental results. The top-right picture is a transient morphology of the PMMA/$E7$ mixture taken under crossed polarizers, showing the nematic line disinclination developed within the irregular-shape domains. The top-left picture is the calculated pattern of the orientational order parameter for a T quench into the metastable liquid–nematic region (e) in Fig. 1, showing nematic ordering within a spinodal–like texture. It is striking to see the resemblance of the calculated and observed domain textures, although the present theory does not take into account the nematic line disinclination.

Another comparison was made between our calculation and the experimental observation of the PMMMA/$E7$ as shown at the bottom row of Fig. 14. The bottom-left picture is the predicted pattern for a T quench into the unstable nematic region (f) in Fig. 1 showing the coexistence of droplet domains and an interconnected texture. The bottom-right picture in Fig. 14 is experimentally observed texture for the $E7$/PMMA mixture. The remarkably similar patterns between the simulated and observed LC domain structures attest to the predictive capability of the present theory.

IV. CONCLUSION

We have demonstrated that the time-dependent Ginzburg–Landau (TDGL, type C) equations in conjunction with the combined Flory–Huggins (FH)/Maier–Saupe (MS) theory, are capable of predicting a rich variety of morphologies of nematic LC/polymer mixtures. The TDGL equations are basically two coupled equations in which a conserved compositional order parameter (i.e., the volume fraction of the liquid crystals) is coupled with a nonconserved orientational order parameter. For the case of a critical T quench into the nematic+liquid region, the spinodal texture eventually breaks down into irregular droplet structures. In the calculation, a plateau region was observed between the intermediate stage ($-1/3$ regime) to the late stage growth (-1 regime) in the temporal evolution of the scattering wave number maximum curve. More importantly, the existence of such a plateau (or inflection) can be verified experimentally in the $E7$/PMMA and $E7$/PMMA–OH mixtures. A T quench into the unstable nematic region confirms the existence of the nematic–liquid spinodal line owing to the development of an interconnected nematic–liquid phase separated texture, reminiscent of spinodal decomposition. The growth of domain structure for a T quench into the metastable liquid–nematic region shows a crossover from the nucleation and growth to the spinodal decomposition mechanism through the coexistence of NG and SD. The predictive capability of the present theory has been demonstrated through the comparison with the experimental observations in the PMMA/$E7$ mixtures.

ACKNOWLEDGMENTS

Support of this work by the National Science Foundation through Grant No. DMR 95-29296 and NSF-STC. Advanced Liquid Crystal Optical Materials (ALCOM) Grant No. 89-20147 is gratefully acknowledged.

[1] J. W. Doane, in *Liquid Crystals: Applications and Uses*, edited by B. Bahadur (World Scientific, Singapore, 1990), Ch. 14, p. 361.
[2] P. S. Drzaic, *Liquid Crystal Dispersions* (World Scientific, Singapore, 1995).
[3] J. West, in *Technological Applications of Dispersions*, edited by R. B. McKay (Marcel Dekker, New York, 1994) p. 345.
[4] C. Shen and T. Kyu, J. Chem. Phys. **102**, 556 (1995).
[5] H.-W. Chiu and T. Kyu, J. Chem. Phys. **103**, 7471 (1995).
[6] T. Kyu and H.-W. Chiu, Phys. Rev. E **53**, 3618 (1996).
[7] H.-W. Chiu and T. Kyu, J. Chem. Phys. **107**, 6859 (1997).
[8] H.-W. Chiu and T. Kyu, J. Chem. Phys. **108**, 3249 (1998).
[9] J. D. Gunton, M. San Miguel, and P. S. Sahni, in *Phase Transitions and Critical Phenomena*, edited by C. Domb and J. L. Lebowitz (Academic, New York, 1983).
[10] P. M. Chaikin and T. C. Lubensky, *Principles of Condensed Matter Physics* (Cambridge University Press, New York, 1995).
[11] P. G. de Gennes, J. Chem. Phys. **72**, 4756 (1980).
[12] P. C. Hohenberg and B. I. Halperin, Rev. Mod. Phys. **49**, 435 (1977).
[13] J. R. Dorgan, J. Chem. Phys. **98**, 9094 (1993).
[14] K. R. Elder, F. Drolet, J. M. Kosterlitz, and M. Grant, Phys. Rev. Lett. **72**, 677 (1994).
[15] P. J. Flory, *Principles of Polymer Chemistry* (Cornell University Press, Ithaca, 1953).
[16] O. Olabisi, L. M. Robeson, and M. T. Shaw, *Polymer–Polymer Miscibility* (Academic, New York, 1979).
[17] W. Maier and A. Saupe, Z. Naturforsch. A **14A**, 882 (1959); *ibid.* **15A**, 287 (1960).
[18] P. G. de Gennes and J. Prost, *The Physics of Liquid Crystals* 2nd Ed. (Oxford Scientific, Oxford University Press, London, 1993).
[19] T. Kyu, I. Ilies, and M. Mustafa, J. Phys. IV **3**, 37 (1993).
[20] T. Kyu, I. Ilies, C. Shen, and Z. L. Zhou, in *Liquid Crystalline Polymer Systems: Technological Advances*, edited by A. I. Isayev, T. Kyu, and S. Z. D. Cheng (A.C.S. Symposium Series # 632, Washington, D.C., 1996), Ch. 13, p. 201.
[21] M. Takenaka and T. Hashimoto, Phys. Rev. E **48**, 47 (1993).
[22] M. Doi and S. F. Edwards, *Theory of Polymer Dynamics* (Academic, New York, 1986).
[23] K. Binder, J. Chem. Phys. **79**, 6387 (1983).